HNPS Advances in Nuclear Physics

Vol 13 (2004)

HNPS2004

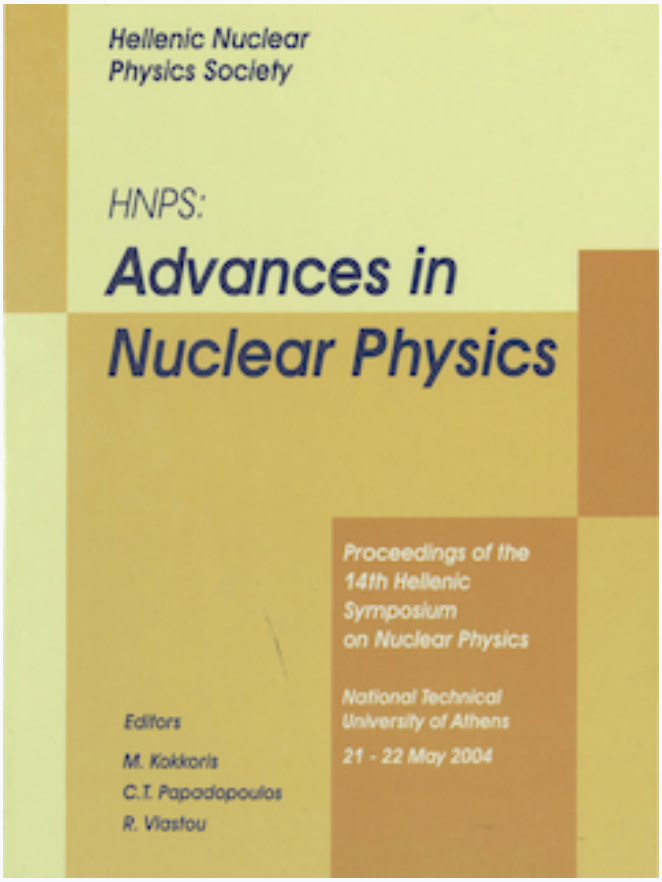

Z(5): Critical Point Symmetry for the Prolate to Oblate Nuclear Shape Phase Transition

Dennis Bonatsos, D. Lenis, D. Petrellis, P. A. Terziev

doi: 10.12681/hnps.2960

Z(5): Critical Point Symmetry for the Prolate to Oblate Nuclear Shape Phase Transition

Dennis Bonatsos [a] D. Lenis [a] D. Petrellis [a] P. A. Terziev [b]

[a] *Institute of Nuclear Physics, N.C.S.R. "Demokritos"*

[b] *Institute for Nuclear Research and Nuclear Energy, Bulgarian Academy of Sciences, 72 Tzarigrad Road, BG-1784 Sofia, Bulgaria*

Abstract

A critical point symmetry for the prolate to oblate shape phase transition is introduced, starting from the Bohr Hamiltonian and approximately separating variables for $\gamma = 30^o$. Parameter-free (up to overall scale factors) predictions for spectra and B(E2) transition rates are found to be in good agreement with experimental data for ^{194}Pt, which is supposed to be located very close to the prolate to oblate critical point, as well as for its neighbours (^{192}Pt, ^{196}Pt).

Key words: Z(5) model; Critical point symmetry; Shape phase transition; Prolate to oblate transition; Triaxial rotator

1 Introduction

Critical point symmetries in nuclear structure are recently receiving considerable attention [1–3], since they provide parameter-free (up to overall scale factors) predictions supported by experimental evidence [4–7]. So far the E(5) [U(5) (vibrational) to O(6) (γ-unstable)] [1,4,5] and the X(5) [U(5) to SU(3) (prolate deformed)] [2,6,7] critical point symmetries have been considered, with the recent addition of Y(5) [3], related to the transition from axial to triaxial shapes. All these critical point symmetries have been constructed by considering the original Bohr equation [8], separating the collective β and γ variables, and making different assumpions about the $u(\beta)$ and $u(\gamma)$ potentials involved.

Furthermore, it has been demonstrated [9] that experimental data in the Hf-Hg mass region indicate the presence of a prolate to oblate shape phase transition, the nucleus ^{194}Pt being the closest one to the critical point. No critical

point symmetry for the prolate to oblate shape phase transition originating from the Bohr equation has been given so far, although it has been suggested [10,11] that the (parameter-dependent) O(6) limit of the Interacting Boson Model (IBM) [12] can serve as the critical point of this transition, since various physical quantities exhibit a drastic change of behaviour at O(6), as they should [13].

In the present work a parameter-free (up to overall scale factors) critical point symmetry, to be called Z(5), is introduced for the prolate to oblate shape phase transition, leading to parameter-free predictions which compare very well with the experimental data for ^{194}Pt.

2 The spectrum

The original Bohr Hamiltonian [8] is

$$H = \frac{\hbar^2}{2B}\left[\frac{1}{\beta^4}\frac{\partial}{\partial\beta}\beta^4\frac{\partial}{\partial\beta} + \frac{1}{\beta^2\sin 3\gamma}\frac{\partial}{\partial\gamma}\sin 3\gamma\frac{\partial}{\partial\gamma} - \right.$$
$$\left. - \frac{1}{4\beta^2}\sum_{k=1,2,3}\frac{Q_k^2}{\sin^2\left(\gamma - \frac{2}{3}\pi k\right)}\right] + V(\beta,\gamma), \qquad (1)$$

where β and γ are the usual collective coordinates, while Q_k (k = 1, 2, 3) are the components of angular momentum and B is the mass parameter.

In the case in which the potential has a minimum around $\gamma = \pi/6$ one can write the last term of Eq. 1 in the form

$$\sum_{k=1,2,3}\frac{Q_k^2}{\sin^2\left(\gamma - \frac{2\pi}{3}k\right)} \approx Q_1^2 + 4(Q_2^2 + Q_3^2) = 4(Q_1^2 + Q_2^2 + Q_3^2) - 3Q_1^2. \quad (2)$$

Using this result in the Schrödinger equation corresponding to the Hamiltonian of Eq. 1, introducing (as in [2]) reduced energies $\epsilon = 2BE/\hbar^2$ and reduced potentials $u = 2BV/\hbar^2$, and assuming [2] that the reduced potential can be separated into two terms, one depending on β and the other depending on γ, i.e. $u(\beta,\gamma) = u(\beta) + u(\gamma)$, the Schrödinger equation can be separated into two equations

$$\left[-\frac{1}{\beta^4}\frac{\partial}{\partial\beta}\beta^4\frac{\partial}{\partial\beta} + \frac{1}{4\beta^2}(4L(L+1) - 3\alpha^2) + u(\beta)\right]\xi_{L,\alpha}(\beta) = \epsilon_\beta\xi_{L,\alpha}(\beta), \quad (3)$$

$$\left[-\frac{1}{\langle\beta^2\rangle\sin 3\gamma}\frac{\partial}{\partial\gamma}\sin 3\gamma\frac{\partial}{\partial\gamma} + u(\gamma)\right]\eta(\gamma) = \epsilon_\gamma\eta(\gamma), \qquad (4)$$

where L is the angular momentum quantum number, α is the projection of the angular momentum on the body-fixed $\hat{x}'$-axis (α has to be an even integer [14]), $\langle\beta^2\rangle$ is the average of β^2 over $\xi(\beta)$, and $\epsilon = \epsilon_\beta + \epsilon_\gamma$.

The total wave function should have the form

$$\Psi(\beta, \gamma, \theta_i) = \xi_{L,\alpha}(\beta)\eta(\gamma)\mathcal{D}^L_{M,\alpha}(\theta_i), \tag{5}$$

where θ_i ($i = 1, 2, 3$) are the Euler angles, $\mathcal{D}(\theta_i)$ denote Wigner functions of them, L are the eigenvalues of angular momentum, while M and α are the eigenvalues of the projections of angular momentum on the laboratory fixed $\hat{z}$-axis and the body-fixed $\hat{x}'$-axis respectively.

Instead of the projection α of the angular momentum on the $\hat{x}'$-axis, it is customary to introduce the wobbling quantum number [14,18] $n_w = L - \alpha$. Inserting $\alpha = L - n_w$ in Eq. 3 one obtains

$$\left[-\frac{1}{\beta^4}\frac{\partial}{\partial\beta}\beta^4\frac{\partial}{\partial\beta} + \frac{1}{4\beta^2}\left(L(L+4) + 3n_w(2L - n_w)\right) + u(\beta)\right]\xi_{L,n_w}(\beta) = \\ = \epsilon_\beta\xi_{L,n_w}(\beta), \tag{6}$$

where the wobbling quantum number n_w labels a series of bands with $L = n_w, n_w + 2, n_w + 4, \ldots$ (with $n_w > 0$) next to the ground state band (with $n_w = 0$) [14].

In the case in which $u(\beta)$ is an infinite well potential

$$u(\beta) = \begin{cases} 0 & \text{if } \beta \leq \beta_W \\ \infty & \text{for } \beta > \beta_W \end{cases}, \tag{7}$$

one can use the transformation [2] $\tilde{\xi}(\beta) = \beta^{3/2}\xi(\beta)$, as well as the definitions [2] $\epsilon_\beta = k_\beta^2$, $z = \beta k_\beta$, in order to bring Eq. 6 into the form of a Bessel equation

$$\frac{d^2\tilde{\xi}}{dz^2} + \frac{1}{z}\frac{d\tilde{\xi}}{dz} + \left[1 - \frac{\nu^2}{z^2}\right]\tilde{\xi} = 0, \tag{8}$$

with

$$\nu = \frac{\sqrt{4L(L+1) - 3\alpha^2 + 9}}{2} = \frac{\sqrt{L(L+4) + 3n_w(2L - n_w) + 9}}{2}. \tag{9}$$

Then the boundary condition $\tilde{\xi}(\beta_W) = 0$ determines the spectrum

$$\epsilon_{\beta;s,\nu} = \epsilon_{\beta;s,n_w,L} = (k_{s,\nu})^2, \qquad k_{s,\nu} = \frac{x_{s,\nu}}{\beta_W}, \tag{10}$$

and the eigenfunctions

$$\xi_{s,\nu}(\beta) = \xi_{s,n_w,L}(\beta) = \xi_{s,\alpha,L}(\beta) = c_{s,\nu}\beta^{-3/2}J_\nu(k_{s,\nu}\beta), \tag{11}$$

where $x_{s,\nu}$ is the sth zero of the Bessel function $J_\nu(z)$, while the constants $c_{s,\nu}$ are determined from the normalization condition $\int_0^\infty \beta^4\xi^2_{s,\nu}(\beta)d\beta = 1$. The notation for the roots has been kept the same as in Ref. [2], while for the energies the notation $E_{s,n_w,L}$ will be used. The ground state band corresponds to $s = 1$, $n_w = 0$. We shall refer to the model corresponding to this solution as Z(5) (which is not meant as a group label), in analogy to the E(5) [1], X(5) [2], and Y(5) [3] models.

The γ-part of the spectrum is obtained from Eq. 4, which can be simply rewritten as

$$\left[-\frac{1}{\langle\beta^2\rangle}\left(\frac{\partial^2}{\partial\gamma^2} + 3\frac{\cos 3\gamma}{\sin 3\gamma}\frac{\partial}{\partial\gamma}\right) + u(\gamma)\right]\eta(\gamma) = \epsilon_\gamma\eta(\gamma). \tag{12}$$

As already mentioned, we consider a harmonic oscillator potential having a minimum at $\gamma = \pi/6$, i.e. $u(\gamma) = \frac{1}{2}c\left(\gamma - \frac{\pi}{6}\right)^2 = \frac{1}{2}c\tilde{\gamma}^2, \qquad \tilde{\gamma} = \gamma - \frac{\pi}{6}$. In the case of $\gamma \approx \pi/6$ the $\cos 3\gamma$ term vanishes and the above equation can be brought into the form

$$\left[-\frac{\partial^2}{\partial\tilde{\gamma}^2} + \frac{1}{2}c\langle\beta^2\rangle\tilde{\gamma}^2\right]\eta(\tilde{\gamma}) = \epsilon_{\tilde{\gamma}}\langle\beta^2\rangle\eta(\tilde{\gamma}), \tag{13}$$

which is a simple harmonic oscillator equation with energy eigenvalues

$$\epsilon_{\tilde{\gamma}} = \sqrt{\frac{2c}{\langle\beta^2\rangle}}\left(n_{\tilde{\gamma}} + \frac{1}{2}\right), \qquad n_{\tilde{\gamma}} = 0, 1, 2, \ldots \tag{14}$$

Similar potentials and solutions in the γ-variable have been considered in [8,19]

The total energy in the case of the Z(5) model is then

$$E(s, n_w, L, n_{\tilde{\gamma}}) = E_0 + A(x_{s,\nu})^2 + Bn_{\tilde{\gamma}}. \tag{15}$$

It should be noticed that in Eq. 13 there is a latent dependence on s, L, and n_w "hidden" in the $\langle\beta^2\rangle$ term. The approximate separation of the β and γ

variables is achieved by considering an adiabatic limit, as in the X(5) case [2,20].

3 B(E2) transition rates

For $\gamma \simeq \pi/6$ the quadrupole operator is given by

$$T^{(E2)}_{\mu} = -\frac{1}{\sqrt{2}} t\beta (\mathcal{D}^{(2)}_{\mu,2}(\theta_i) + \mathcal{D}^{(2)}_{\mu,-2}(\theta_i)). \tag{16}$$

where t is a scale factor. After the insertion of the symmetrized wave function, B(E2) transition rates are given by

$$B\left(E2; L_i\alpha_i \rightarrow L_f\alpha_f\right) = \frac{5t^2}{32\pi} \frac{I^2_\beta(s_i, L_i, \alpha_i, s_f, L_f, \alpha_f)}{(1+\delta_{\alpha_i,0})(1+\delta_{\alpha_f,0})} \times$$
$$\times \left[(L_i 2 L_f|\alpha_i 2\alpha_f) + (L_i 2 L_f|\alpha_i - 2\alpha_f) + (-1)^{L_i}(L_i 2 L_f| - \alpha_i 2\alpha_f)\right]^2 \tag{17}$$

(For details on the calculation and numerical results, see ref. [26].)

One can easily see that the Clebsch–Gordan coefficients (CGCs) appearing in this equation impose a $\Delta\alpha = \pm 2$ selection rule. Indeed, the first CGC is nonvanishing only if $\alpha_i + 2 = \alpha_f$, while the second CGC is nonvanishing only if $\alpha_i - 2 = \alpha_f$. The third CGC is nonvanishing only if $\alpha_i + \alpha_f = 2$, which can be valid only in a few special cases. The angular part of this equation is equivalent to the results obtained in [14].

It should also be noticed that quadrupole moments vanish, because of the $\Delta\alpha = \pm 2$ selection rule, since in the relevant matrix elements of the quadrupole operator one should have $\alpha_i = \alpha_f$.

4 Numerical results

The lowest bands of the Z(5) model are given in Table 1. The notation L_{s,n_w} is used. All levels are measured from the ground state, $0_{1,0}$, and are normalized to the first excited state, $2_{1,0}$. The ground state band is characterized by $s = 1$, $n_w = 0$, while the even and the odd levels of the γ_1-band are characterized by $s = 1$, $n_w = 2$, and $s = 1$, $n_w = 1$ respectively. The β_1-band is characterized by $s = 2$, $n_w = 0$. All these bands are characterized by $n_{\tilde{\gamma}} = 0$, and, as seen from Eq. 15, are parameter free. The fact that the γ_1-band is characterized by

Table 1
Energy levels of the Z(5) model (with $n_{\tilde{\gamma}} = 0$), measured from the $L_{s,n_w} = 0_{1,0}$ ground state and normalized to the $2_{1,0}$ lowest excited state.

s, n_w	1,0	1,2	2,0		1,1
L				L	
0	0.000		3.913		
2	1.000	1.837	5.697	3	2.597
4	2.350	4.420	7.962	5	4.634
6	3.984	7.063	10.567	7	6.869
8	5.877	9.864	13.469	9	9.318
10	8.019	12.852	16.646	11	11.989
12	10.403	16.043	20.088	13	14.882
14	13.024	19.443	23.788	15	18.000
16	15.878	23.056	27.740	17	21.341
18	18.964	26.884	31.942	19	24.905
20	22.279	30.928	36.390	21	28.691

$n_{\tilde{\gamma}} = 0$ is not surprising, since this is in general the case in the framework of the rotation-vibration model [21].

5 Comparison to experiment

Several energy levels and B(E2) transition rates predicted by the Z(5) model are compared in Table 2 to the corresponding experimental quantities of ^{194}Pt [22], which has been suggested [9] to lie very close to the prolate to oblate critical point. Its neighbours, ^{192}Pt [23] and ^{196}Pt [24], which demonstrate quite similar behaviour, are also shown. Not only the levels of the ground state band are well reproduced (below the backbending), but in addition the bandheads of the γ_1-band and the β_1-band are very well reproduced, without involving any free parameter. The staggering of the theoretical levels within the γ_1-band is quite stronger than the one seen experimentally, as it is expected [17] for models related to the triaxial rotator [14–16].

The main features of the B(E2) transition rates are also well reproduced. As far as the transitions from the γ_1-band to the ground state band are concerned, the transitions $L_{1,2} \to L_{1,0}$ are strong, while the transitions $(L+2)_{1,2} \to L_{1,0}$, which are forbidden in the Z(5) framework, are weaker by two or three orders of magnitude.

Table 2
Comparison of the Z(5) predictions for energy levels (left part) and B(E2) transition rates (right part) to experimental data for ^{192}Pt [23], ^{194}Pt [22], and ^{196}Pt [24].

L_{s,n_w}	Z(5)	^{192}Pt	^{194}Pt	^{196}Pt	$L^{(i)}_{s,n_w}$	$L^{(f)}_{s,n_w}$	Z(5)	^{192}Pt	^{194}Pt	^{196}Pt
$4_{1,0}$	2.350	2.479	2.470	2.465	$4_{1,0}$	$2_{1,0}$	1.590	1.559	1.724	1.476
$6_{1,0}$	3.984	4.314	4.299	4.290						
$8_{1,0}$	5.877	6.377	6.392	6.333	$4_{1,2}$	$2_{1,2}$	0.736		0.446	0.715
$10_{1,0}$	8.019	8.624		8.558	$6_{1,2}$	$4_{1,2}$	1.031			1.208
$2_{1,2}$	1.837	1.935	1.894	1.936	$3_{1,1}$	$2_{1,2}$	2.171	1.786		
$4_{1,2}$	4.420	3.795	3.743	3.636						
$6_{1,2}$	7.063	5.905	5.863	5.644	$2_{1,2}$	$0_{1,0}$	0.000	0.009	0.006	0.0004
					$2_{1,2}$	$2_{1,0}$	1.620	1.909	1.805	
$3_{1,1}$	2.597	2.910	2.809	2.854	$4_{1,2}$	$2_{1,0}$	0.000		0.004	0.014
$5_{1,1}$	4.634	4.682	4.563	4.526	$4_{1,2}$	$4_{1,0}$	0.348		0.406	
$7_{1,1}$	6.869	6.677			$6_{1,2}$	$4_{1,0}$	0.000			0.012
$0_{2,0}$	3.913	3.776	3.858	3.944						

References

[1] F. Iachello, Phys. Rev. Lett. 85 (2000) 3580.

[2] F. Iachello, Phys. Rev. Lett. 87 (2001) 052502.

[3] F. Iachello, Phys. Rev. Lett. 91 (2003) 132502.

[4] R. F. Casten and N. V. Zamfir, Phys. Rev. Lett. 85 (2000) 3584.

[5] N. V. Zamfir *et al.*, Phys. Rev. C 65 (2002) 044325.

[6] R. F. Casten and N. V. Zamfir, Phys. Rev. Lett. 87 (2001) 052503.

[7] R. Krücken *et al.*, Phys. Rev. Lett. 88 (2002) 232501.

[8] A. Bohr, Mat. Fys. Medd. K. Dan. Vidensk. Selsk. 26 (1952) no. 14.

[9] J. Jolie and A. Linnemann, Phys. Rev. C 68 (2003) 031301.

[10] J. Jolie, R. F. Casten, P. von Brentano, and V. Werner, Phys. Rev. Lett. 87 (2001) 162501.

[11] J. Jolie, P. Cejnar, R. F. Casten, S. Heinze, A. Linnemann, and V. Werner, Phys. Rev. Lett. 89 (2002) 182502.

[12] F. Iachello and A. Arima, The Interacting Boson Model, Cambridge University Press, Cambridge, 1987.

[13] V. Werner, P. von Brentano, R. F. Casten, and J. Jolie, Phys. Lett. B 527 (2002) 55.

[14] J. Meyer-ter-Vehn, Nucl. Phys. A 249 (1975) 111.

[15] A. S. Davydov and G. F. Filippov, Nucl. Phys. 8 (1958) 237.

[16] A. S. Davydov and V. S. Rostovsky, Nucl. Phys. 12 (1959) 58.

[17] N. V. Zamfir and R. F. Casten, Phys. Lett. B 260 (1991) 265.

[18] A. Bohr and B. R. Mottelson, Nuclear Structure, Benjamin, New York, 1975, Vol. II.

[19] A. S. Davydov, Nucl. Phys. 24 (1961) 682.

[20] R. Bijker, R. F. Casten, N. V. Zamfir, and E. A. McCutchan, Phys. Rev. C 68 (2003) 064304.

[21] W. Greiner and J. A. Maruhn, Nuclear Models, Springer, Berlin, 1996.

[22] E. Browne and B. Singh, Nucl. Data Sheets 79 (1996) 277.

[23] C. M. Baglin, Nucl. Data Sheets 84 (1998) 717.

[24] C. Zhou, G. Wang, and Z. Tao, Nucl. Data Sheets 83 (1998) 145.

[25] D. Bonatsos, D. Lenis, N. Minkov, D. Petrellis, P. P. Raychev, and P. A. Terziev, Phys. Lett. B, in press. nucl-th/0312121.

[26] D. Bonatsos, D. Lenis, D. Petrellis, and P. A. Terziev, nucl-th/0402087.